ISSN 2181-8622

Manufacturing technology problems

Scientific and Technical Journal Namangan Institute of Engineering and Technology

INDEX COPERNICUS INTERNATIONAL

Google Scholar Crossref doi SLIB.UZ Scientific library of Uzbekistan

Volume 11
Issue 1
2026

NamMTI ILMIY-TEXNIKA JURNALI TAHRIR HAY'ATI A'ZOLARI

HYDROTHERMAL SYNTHESIS OF KA (LTA-TYPE) ZEOLITE FROM ANGREN KAOLIN: STRUCTURAL, MORPHOLOGICAL, AND ADSORPTION CHARACTERIZATION

MUKHAMMADJONOV MIRJALOL
PhD student, Namangan State Technical University, Namangan, Uzbekistan
Phone.: (0891) 323-9909, E-mail.: mm.muxammadjonov@gmail.com
**Corresponding author*

RAKHMATKARIEVA FIRUZA
Professor, Institute of General and Inorganic Chemistry of Academy of Sciences of the Republic of Uzbekistan, Tashkent, Uzbekistan
Phone.: (0899) 819-0323, E-mail.: rakhfiruza@gmail.com

OYDINOV MUKHLIS
PhD, Tashkent State Medical University, Tashkent, Uzbekistan
Phone.: (0890) 337-7607, E-mail.: muxlisoydinov107@gmail.com

Abstract: This study explores Angren kaolin as a low-cost local raw material for the synthesis of KA zeolite (LTA-type). A multi-step activation process using oxalic acid was applied to remove impurities and enhance reactivity. Hydrothermal synthesis yielded highly crystalline KA zeolite, whose structural and adsorption properties were thoroughly investigated. XRD analysis confirmed the formation of an ordered crystalline lattice, while FTIR spectra revealed characteristic Si–O–Si and Al–O vibrations and the presence of double four-ring (D4R) units typical of LTA-type zeolites. BET and DFT analyses demonstrated a well-developed porous structure and strong adsorption capacity: BET surface area was 8.475 m²/g, DFT surface area 19.575 m²/g, maximum adsorption volume 149.00 cc/g, and average pore diameter 121.955 Å. These findings confirm the high hydrophilicity and efficiency of KA zeolite as an adsorbent. The study provides a scientific basis for utilizing Angren kaolin in zeolite synthesis and highlights the strategic importance of local resources for future industrial-scale applications.

Keywords: Kaolin, porous materials, zeolite, spectroscopy, hydrothermal method, crystal, X-ray, diffraction.

Introduction. Zeolites are crystalline aluminosilicate materials characterized by a three-dimensional framework composed of large cavities and channels. Due to this unique structure, zeolites exhibit ion-exchange, adsorption, and catalytic properties. Zeolites are widely used as catalysts, gas separation materials, and ion-exchange agents. In the petrochemical industry, zeolites serve as catalysts in industrial processes such as isomerization, cracking, and hydrocarbon synthesis [1–4]. The most efficient method for large-scale synthesis of zeolites is the hydrothermal method. This process is typically carried out at temperatures below 300 °C and under autogenous pressure generated in an autoclave [5–6].

In the hydrothermal synthesis process, NaOH or KOH is commonly used as a mineralizing agent, while the cations of alkali and alkaline earth metals act as structure-directing agents. An increase in the pH level of the mixture accelerates the dissolution of amorphous aluminosilicates and leads to the formation of silicate, aluminate, and aluminosilicate species in high concentrations. Such conditions promote rapid nucleation and crystal growth, thereby facilitating the formation of an ordered crystalline structure. At the same time, crystallization time is considered one of the most important parameters

of the synthesis process. If insufficient time is provided, crystals may form with poorly defined morphology or the product may remain completely amorphous. Conversely, an optimal crystallization time ensures the formation of zeolites with a high degree of crystallinity and stable morphology [7–8].

In the synthesis of LTA-type zeolites, parameters such as the initial composition of the reaction mixture, temperature, pressure, and crystallization time directly influence the crystallinity, particle morphology, and size of the obtained product [9–10]. These factors determine the kinetics and thermodynamics of the synthesis process and ultimately define the quality characteristics of the resulting zeolite. Currently, about 20 different types of zeolites are produced on an industrial scale. The global annual demand for zeolites is estimated at 1.7–2 million tons, of which approximately 73% corresponds to Zeolite A (LTA-type zeolite) [11–13]. This high share is explained by the excellent performance of Zeolite A in ion-exchange, adsorption, and catalytic processes. Zeolite A (LTA-type zeolite) is distinguished by its well-defined crystal framework, high hydrophilicity, and selectivity toward water molecules. Its LTA structure, consisting of sodalite units and large cages, enables the ordered diffusion of molecules through the framework. Due to its high hydrophilicity, Zeolite A strongly adsorbs water molecules and is effectively used in drying processes. In addition, it has wide industrial applications in gas separation, purification, and ion-exchange processes, making it one of the most promising adsorbents in practical applications [14–15].

Furthermore, the multistage strategy involving oxalic acid treatment during the activation of kaolin has not yet been sufficiently optimized. As a result, the structural and adsorption properties of the synthesized product have not been comprehensively compared with those of commercial Linde A zeolite or with results reported in recent scientific literature. Therefore, the main objective of this study is to conduct an in-depth investigation of the synthesis of KA (LTA-type) zeolite from Angren kaolin.

Research Objects and Methods. In this study, Angren kaolin was selected as the main aluminosilicate source for the synthesis of LTA-type zeolite. It naturally contains a high amount of aluminum and silicon oxides. This raw material is considered an environmentally friendly, economically affordable, and readily available source. Initially, the kaolin sample was ground in a ball mill to achieve a high level of mechanical activation. The sample was then prepared for the purification stage. At this stage, iron compounds that could interfere with the synthesis process were removed.

During the preliminary purification of kaolin, oxalic acid ($H_2C_2O_4$), one of the organic acids, was selected. The main reason for this choice is the strong complex-forming ability of oxalic acid with Fe^{3+} ions, which enables the selective removal of iron oxides. The ground kaolin was treated with a 0.5 M oxalic acid solution at a temperature of 100 °C. Under these conditions, iron, titanium, and other undesirable impurities are transferred into the solution, resulting in a significant purification of the chemical composition of the kaolin [16–17].

The primary purpose of oxalic acid treatment is the selective removal of iron oxides (Fe_2O_3, Fe_3O_4), titanium dioxide (TiO_2), and other undesirable impurities present in

kaolin. These impurities negatively affect zeolite crystallization, particularly by reducing the nucleation rate, disrupting the ordering of the crystal framework, and limiting adsorption properties. Oxalic acid forms highly stable $Fe(C_2O_4)_3^{3-}$ complexes with Fe^{3+} ions, which allows iron to be transferred from the solid phase to the liquid phase. In addition, treatment with oxalic acid helps optimize the Si/Al ratio.

During the solution treatment process, oxalic acid gradually dissociates into ions in two stages:

1. **First dissociation stage:**

$$H_2C_2O_4 \rightarrow H^+ + HC_2O_4^-$$

2. **Seconddissociationstage:**

$$HC_2O_4^- \rightarrow H^+ + C_2O_4^{2-}$$

The resulting $HC_2O_4^-$ and $C_2O_4^{2-}$ ions effectively dissolve iron oxides by complexing them and transferring them into the aqueous phase. The reaction proceeds as follows:

$$Fe_2O_3 + H^+ + 5HC_2O_4^- \rightarrow 2Fe(C_2O_4)_2^{2-} + 3H_2O + 2CO_2$$

After the removal of iron and other impurities, the silicate and aluminate composition of kaolin becomes balanced, which ensures the Si/Al ≈ 1 ratio required for LTA-type zeolites. As a result, an increase in zeolite crystallinity, a more ordered particle morphology, and improved adsorption capacity are observed. Experimental results show that samples treated with oxalic acid exhibit a higher degree of crystallinity, a well-defined phase structure, and improved adsorption properties compared with commercial Linde KA zeolite. This confirms the importance of oxalic acid as a stable, environmentally safe, and selective purification reagent in the zeolite synthesis process.

After the treatment process, the samples were cooled to room temperature, filtered, and dried again at 100 °C. The initial chemical composition of Angren kaolin is presented in **Table 1**, while the composition of the main oxides in the purified sample is given in **Table 2**.

Table 1. Chemical composition of Angren kaolin (%)

Component	Al_2O_3	CaO	Fe_3O_4	K_2O	MgO	Na_2O	P_2O_5	SiO_2	TiO	Other components
Content (%)	31.2	1.24	0.80	0.283	0.723	4.69	0.07	48.9	0.45	11.674

Thermal treatment and metakaolin formation. The kaolin mineral was subjected to thermal activation, during which the removal of OH^- groups from its crystal framework resulted in the formation of metakaolin. This process was carried out in a muffle furnace at a temperature range of **500–800 °C** for **6 hours**.

Table 2. Chemical composition of purified kaolin (%)

Component	Al_2O_3	Na_2O	SiO_2	Fe_3O_4	Other components
Content (%)	37.4	5.5	55.6	0.1	1.4

Gel preparation and hydrothermal synthesis. Metakaolin was used as the raw material in the synthesis process. Kaolin was calcined at 700 °C for 4 hours to obtain amorphous metakaolin. For the synthesis, 1.00 g of metakaolin was mixed with a 2 M sodium hydroxide (NaOH) solution. The mixture was stirred with a magnetic stirrer to form a homogeneous suspension. At this stage, sodium hydroxide activates the amorphous structure of metakaolin, creating the necessary conditions for zeolite formation. The pH of the resulting gel was maintained in the range of 12–13, and the prepared suspension was transferred into a 25 mL Teflon-lined autoclave. Hydrothermal synthesis was conducted at 100 °C under autogenous pressure for 28 hours, during which nucleation and crystal growth of NaA zeolite occurred.

After synthesis, the product was removed from the autoclave, filtered under vacuum, and washed 3–4 times with distilled water to completely remove excess alkali. Washing was continued until the solution reached a pH ≈ 7. As a result, NaA zeolite with a crystalline structure was obtained.

The obtained NaA zeolite sample was then subjected to ion-exchange treatment. For this purpose, 50 mL of 1 M KCl solution was prepared, and the NaA zeolite was washed three times with this solution. During this process, Na^+ ions were exchanged with K^+ ions, resulting in the formation of KA zeolite. The ion-exchange process chemically modified the zeolite, altering its physicochemical properties. The final KA zeolite sample was dried at 80 °C for 12 hours (Figure 1). After drying, a white crystalline KA zeolite was obtained, characterized by its ion-exchange capacity and adsorption properties.

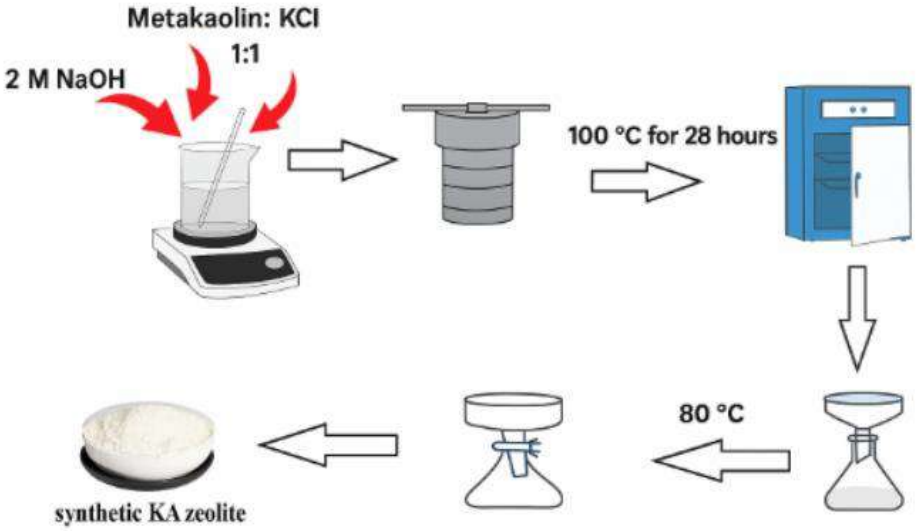

Figure 1. Schematic diagram of the synthesis of K-A zeolite by the hydrothermal method

The crystalline structure (XRD), morphology, and chemical composition of the obtained products were analyzed using spectroscopic techniques, scanning electron microscopy (SEM), and energy-dispersive X-ray spectroscopy (EDS), and relevant conclusions were drawn. To evaluate the adsorption properties of the zeolite samples, water adsorption and nitrogen adsorption measurements were conducted using BET analysis. These results indicate that KA zeolite possesses a highly developed porous structure and can be effectively utilized as a molecular sieve.

The KA-type zeolite sample synthesized via hydrothermal treatment from Angren kaolin, as well as a comparative LTA-type zeolite sample, were studied. The synthesis process involved the calcination of kaolin to metakaolin, followed by crystallization under hydrothermal conditions. During hydrothermal synthesis, the pH, temperature (within 90–100 °C), and time parameters were strictly controlled, which played a crucial role in the formation of the crystal structure and in achieving a high yield of the final product. The obtained samples were analyzed by X-ray diffraction (XRD). XRD measurements were performed using a SHIMADZU XRD-6100 diffractometer with a Cu-Kα radiation source (λ = 1.5406 Å), operating at 40 kV and 30 mA. The resulting diffraction patterns were compared with data from the International Centre for Diffraction Data (ICDD) and other global crystal structure databases. This analysis confirmed that the chemical formula of KA zeolite is $Al_{10}H_{72}K_{4.63}Na_6O_{91.32}Si_{25.38}$.

Energy-dispersive X-ray spectroscopy (EDS) was employed to evaluate the elemental composition. The results showed that KA zeolite contains O – 51.2%, Si – 25%, Al – 10%, K – 6.3%, Na – 4.8%, and H – 2.5%. The degree of crystallinity and amorphous content were calculated from the integral areas of the XRD diffractograms, revealing that KA zeolite has a crystallinity of 70.91% and an amorphous content of 29.09%. This is attributed to the presence of a mixture of phases and amorphous components formed during synthesis (Figure 2).

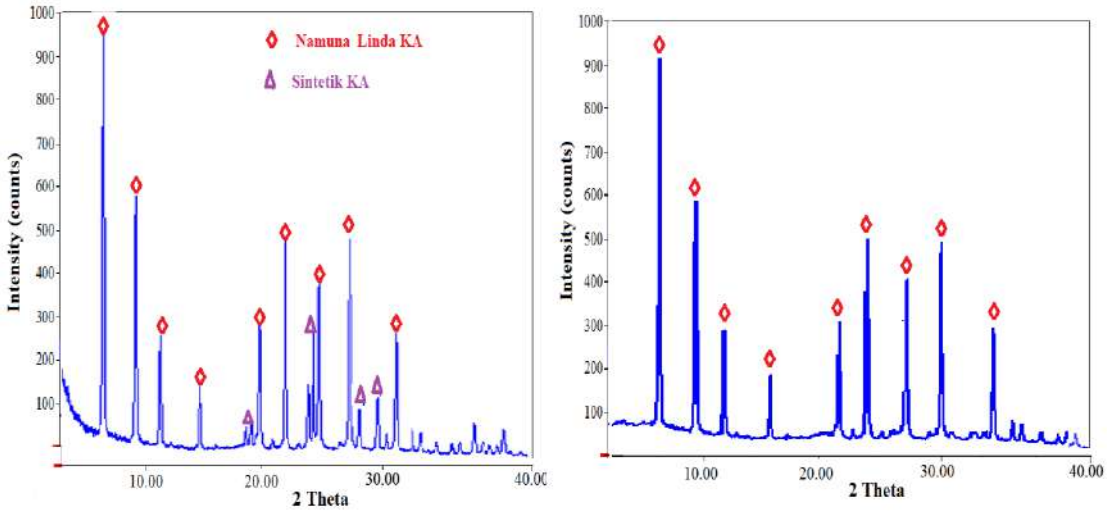

Figure 2. XRD patterns of the synthesized KA and LTA zeolite crystals

Morphological studies using optical and electron microscopy showed that KA zeolite crystals generally exhibit anisotropic shapes and are composed of crystallites growing in various orientations.

The crystal size and spatial orientation of the zeolite are key parameters determining its catalytic and adsorption properties. Therefore, optimizing the porous structure and channel orientation of the synthesized zeolites enhances their catalytic and adsorption efficiency.

The infrared (IR) absorption and transmission properties of the synthesized KA zeolite samples were analyzed using a Bruker ALPHA II FTIR spectrometer. Measurements were performed in the 4000–400 cm^{-1} range, and the main vibrational bands were identified and assessed for their relevance to the zeolite structure.

FTIR spectral analysis revealed a sharp absorption band at 465.84 cm^{-1}, corresponding to the bending vibrations of Si–O or Al–O bonds in the KA zeolite. A distinct vibrational band observed at 673.13 cm^{-1} is attributed to symmetric Si–O–Si vibrations. In addition, asymmetric stretching vibrations of T–O–T (T = Si or Al) bonds were detected with relatively low intensity. A high-intensity peak at 1006.19 cm^{-1} corresponds to the asymmetric stretching vibrations of Si–O–Si bonds, indicating that asymmetric stretching vibrations are more pronounced than bending vibrations in the Si–O–Si framework.

For the LTA-type zeolite structure, the characteristic secondary four-membered rings (D4R – Double Four Ring) were observed at 556.79 cm^{-1}. These structural units act as fundamental building blocks of the zeolite and contribute to the stability of its crystalline framework.

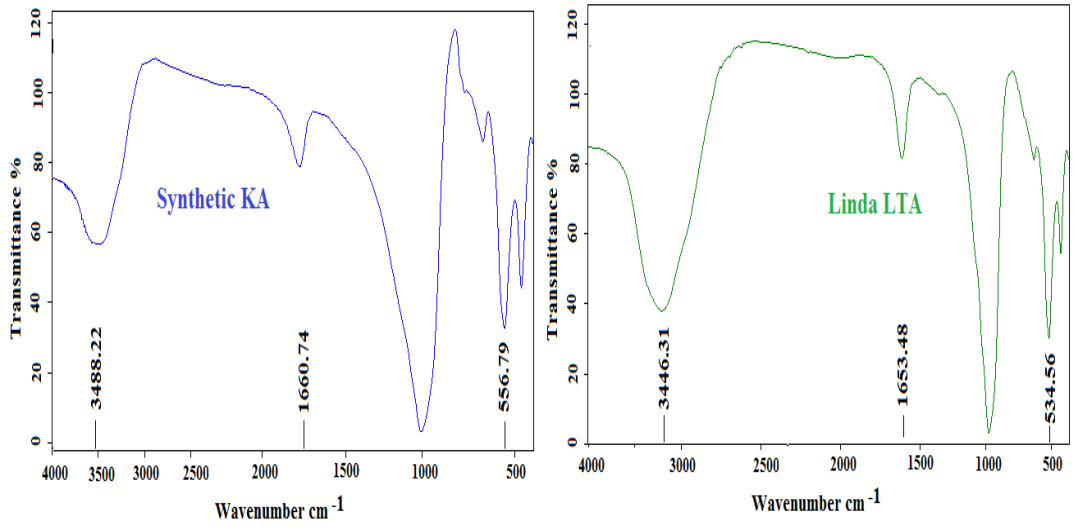

Figure 3. FTIR spectra of the synthesized KA and LTA zeolite crystals

FTIR Analysis of Water Molecules in KA Zeolite. The FTIR spectral analysis of KA zeolite samples revealed two significant infrared regions associated with water molecules. In zeolite structures, water molecules are coordinated with cations, and their

hydrogen atoms form partial hydrogen bonds with the framework oxygen ions. The degree of interaction between water molecules and cations or framework oxygen ions is directly related to the openness of the zeolite structure. A broad absorption band at **3488.22 cm^{-1}** corresponds to hydrogen (OH) vibrations, indicating hydrogen bonding between water molecules and framework oxygen ions. An intense absorption band at **1660.74 cm^{-1}** is attributed to the bending vibrations of water molecules. These strong and well-defined vibrational bands confirm the highly **hydrophilic nature** and good hydration of KA zeolite. The intensity of these bands is significantly higher compared with the amorphous phase, indicating that the main mass of the prepared gel corresponds to the KA-type crystalline structure.

The FTIR spectrum of the synthesized KA zeolite confirms its structural stability and chemical composition, which is similar to that of LTA-type zeolites. Compared with nanosized Linde A zeolite obtained via hydrothermal synthesis, the KA zeolite shows a high-intensity peak at ≈1000 cm^{-1}, corresponding to the asymmetric stretching vibrations of T–O–T bonds. Additionally, a peak at 472.0 cm^{-1} corresponds to Si–O vibrations, and other asymmetric stretching vibrations are observed at lower intensities. A broad absorption band at 3446.31 cm^{-1} further indicates hydrogen bonding between OH groups and framework oxygen ions (Figure 3). These FTIR results confirm that the synthesized KA zeolite has a fully developed crystalline structure, and its constituent elements and secondary building units are characteristic of LTA-type zeolites.

BET Analysis of the Synthesized KA Zeolite **Nitrogen adsorption** measurements provided critical information regarding the **microporous structure, surface area, and pore volume** of the synthesized KA zeolite. Adsorption–desorption isotherms obtained using BET and DFT models confirm the material's efficiency as an adsorbent.

Adsorption isotherm analysis.The adsorption–desorption isotherms of nitrogen gas at 77.35 K reveal a distinct hysteresis loop, indicating capillary condensation and the "memory effect" of the porous structure. At low relative pressures ($P/P_0 < 0.2$), the adsorption curve rises slowly, corresponding to monolayer adsorption on the surface. In the medium pressure range ($P/P_0 \approx 0.2–0.75$), the adsorption volume increases steadily, reflecting the filling of micropores. At high relative pressures ($P/P_0 > 0.75$), the curve rises sharply, reaching a maximum adsorption volume of 149.00 cc/g, where capillary condensation occurs in the micropores. The desorption curve lies below the adsorption curve, indicating slower gas release from the pores compared with adsorption (Figure 4). This hysteresis confirms incongruent desorption and reflects the complexity of pore shapes, sizes, and connectivity. The nitrogen molecule has a diameter of 3.54 Å, molecular weight of 28.013 g/mol, and cross-sectional area of 16.200 Å^2, consistent with the microporous structure of KA zeolite. Thermal activation and a liquid density of 0.808 g/cc during experiments enhance the accuracy of adsorption measurements.

BET analysis.Using the MBET model, the BET slope was 324.535 1/g, intercept 86.37 1/g, C constant 4.758, and correlation coefficient 0.9757, indicating excellent model fitting. The MBET surface area was calculated as 8.475 m^2/g. This indicates that nitrogen (N_2) adsorption is highly limited in KA zeolite because K^+-exchanged A-type zeolites

selectively adsorb oxygen rather than nitrogen. Consequently, in O_2/N_2 gas mixtures, KA zeolite adsorbs oxygen while nitrogen primarily passes through, with adsorption occurring only on a limited portion of the surface (Table 3).

Table 3. N_2 adsorption analysis of different zeolite types

Zeolite type	Cation	N_2 adsorption capacity	O_2/N_2 selectivity
NaA (4A)	Na^+	Average	Low
KA (3A-K)	K^+	Very low	Very high (relative to O_2)
CaA (5A)	Ca^{2+}	Average	Average
13X	Na^+	High (physical adsorption)	Low

DFT Analysis and Pore Structure. The results obtained from the **DFT model** provided a deeper insight into the pore structure of the KA zeolite. According to the analysis, the **pore volume** was **0.153 cc/g**, the **surface area** was **19.575 m²/g**, and the **average pore diameter** was **121.955 Å**. These results confirm that KA zeolite possesses **wide-diameter pores** along with a well-developed **microporous structure**.

The pore diameter distribution curves indicate monolayer Langmuir-type behavior during the adsorption process. The adsorption isotherms, together with BET and DFT analyses, demonstrate the potential of KA zeolite as a highly efficient adsorbent. Its microporous structure, selective adsorption properties, low energy consumption, and environmental safety make it an ideal material for sustainable industrial processes. These findings suggest that KA zeolite can be widely applied in water purification, gas separation, and greenhouse gas capture technologies.

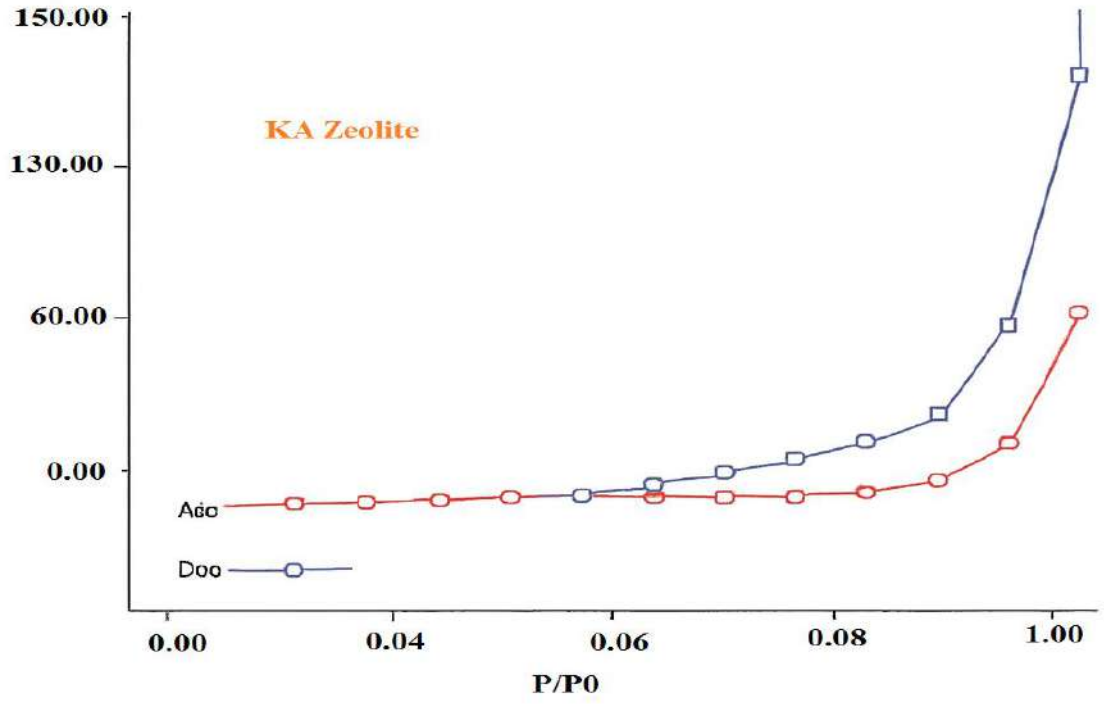

Figure 4. N_2 adsorption isotherm of the synthesized KA zeolite molecular sieves

Advantages and Limitations of Industrial-Scale Zeolite Production from Kaolin

The advantages of industrial-scale zeolite production from kaolin include the low cost and local availability of raw materials. Zeolite A, as a widely used material, finds applications in detergents, gas separation, and catalytic processes. Additionally, the synthesis process contributes to waste reduction and ensures environmental sustainability.

However, the hydrothermal process is energy-intensive, involves multiple operational steps, and requires complex production lines, which are considered as limitations. Further research is needed to reduce crystallization time and minimize reagent consumption.

Overall, zeolite synthesis from kaolin is economically efficient and promising, distinguished by inexpensive raw materials, abundant resources, and environmental safety. Nevertheless, when implementing this process at an industrial scale, careful evaluation of technological steps, energy consumption, and capital costs is necessary.

Conclusion: The selection of Angren kaolin as a raw material, due to its low cost, local availability, and high content of Al_2O_3 and SiO_2, was a key advantage of this study. The treatment with oxalic acid selectively removed iron and other undesirable impurities, optimizing the chemical composition of the kaolin. This adjustment ensured the required Si/Al ≈ 1 ratio for zeolite crystallization, facilitating the formation of high-quality crystalline structures.

During the hydrothermal synthesis, kaolin was calcined to metakaolin, and crystallization was achieved with the assistance of NaOH. XRD diffractograms confirmed that the KA zeolite possessed a well-ordered crystalline framework. The crystallinity reached 70.91%, while the amorphous fraction was 29.09%, indicating that the synthesis was conducted under optimal conditions and resulted in a highly crystalline product.

FTIR spectral analysis provided detailed insight into the structural characteristics of KA zeolite. Peaks in the 465–673 cm^{-1} range corresponded to Si–O–Si and Al–O vibrations, while the 556 cm^{-1} band indicated the presence of secondary double four-ring (D4R) units, characteristic of LTA-type zeolites. A high-intensity peak at 1006 cm^{-1} was attributed to asymmetric Si–O–Si stretching vibrations, and bands at 3488 cm^{-1} and 1660 cm^{-1} reflected the hydrogen bonding and bending vibrations of water molecules, confirming the highly hydrophilic nature of the KA zeolite.

BET and DFT analyses elucidated the pore structure and adsorption properties of KA zeolite. The BET surface area was 8.475 m^2/g, indicating low N_2 adsorption capacity, which can be attributed to the O_2 selectivity of the A-type zeolite exchanged with K^+ ions. Accordingly, KA zeolite effectively adsorbs oxygen molecules in O_2/N_2 separation processes. The DFT model provided deeper insights, revealing a surface area of 19.575 m^2/g, pore volume of 0.153 cc/g, and an average pore diameter of 121.955 Å, confirming the presence of a well-developed microporous structure with wide-diameter pores.

Overall, the results demonstrate that using Angren kaolin is environmentally safe, economically efficient, and strategically significant. The synthesized KA zeolite shows

strong potential as an efficient adsorbent for gas separation, water purification, and various industrial applications.

References:

1. M. Ghasemi, A. M. Rashidi, H. Fazlollahi, S. Mohammadi, "Synthesis of Zeolite 4A from Natural Kaolin for Adsorption of Heavy Metals," Microporous and Mesoporous Materials 295 (2020) 109953.

2. V. C. Eluwa, E. O. Ofoegbu, A. U. Idoko, "Hydrothermal Synthesis of Zeolite A from Aloji Kaolin: Characterization and Performance Evaluation," Journal of Materials Science Research and Reviews 18 (2024) 55-65.

3. A. Abubakar, M. Musa, S. Abdulkarim, "Hydrothermal Synthesis and Characterization of Zeolite A from Kaolinitic Clay," Nanochemistry Research 8 (2023) 89-101.

4. N. Gougazeh, M. Buhl, "Synthesis and Characterization of Zeolite A by Hydrothermal Transformation of Natural Jordanian Kaolin," Clay Minerals 55 (2020) 150-162.

5. P. Wang, J. Liu, R. Zhang, "Hydrothermal Synthesis of Zeolite 4A from Low-Grade Kaolin and its Adsorptive Properties," Applied Clay Science 170 (2019) 40-47.

6. M. C. Hernandez, L. M. Contreras, "Effect of NaOH Concentration on Hydrothermal Synthesis of Zeolite A from Kaolin," Journal of the European Ceramic Society 42 (2022) 3570-3578.

7. Li, X., Wang, Y., & Chen, J. (2021). *Hydrothermal synthesis of LTA zeolite from natural kaolin: Optimization and characterization*. Microporous and Mesoporous Materials, 323, 111–120.

8. Zhang, Q., Liu, H., & Zhao, Y. (2022). *Comparative study of Linde Type A zeolite synthesized from different kaolin sources*. Journal of Materials Science, 57(14), 9234–9248.

9. L. Zhang, X. Han, J. Chen, "Crystallization Mechanism of Zeolite A Synthesized from Kaolin-Derived Metakaolin," Microporous and Mesoporous Materials 322 (2021) 111163.

10. E. Alkan, A. Sahin, "Utilization of Kaolin Waste for the Production of Zeolite 4A," Journal of Cleaner Production 275 (2020) 122954.

11. R. Becerra, J. P. Parra, "Effect of Crystallization Time on the Morphology of Zeolite A Synthesized from Kaolinite," Journal of Sol-Gel Science and Technology 103 (2022) 349-360.

12. Y. T. Nguyen, M. A. Pham, "Low-Temperature Hydrothermal Synthesis of Zeolite A from Metakaolin," Advanced Powder Technology 33 (2022) 103615.

13. Al-Mamun, M., & Lee, J. (2023). *Advances in sustainable zeolite synthesis: Local raw materials and green activation strategies*. Chemical Engineering Journal, 451, 138–149.

14. Petrova, D., Ivanov, K., & Dimitrov, A. (2024). *Adsorption properties of LTA zeolite compared with commercial Linde A: A five-year perspective*. Journal of Environmental Chemical Engineering, 12(3), 109–118.

15. J. Randrianandraina, M. Badawi, B. Cardey, M. Grivet, J.-E. Groetz, C. Ramseyer, F. T. Anzola, C. Chambelland, D. Ducret, *"Adsorption of water in Na-LTA*

zeolites: An ab initio molecular dynamics investigation," Physical Chemistry Chemical Physics, 23 (2021) 19145–19156.

16. J. Pan, B. Wang, S. Liu, S. Liu, W. Yan, *"Synthesis and Application of LTA Zeolite for the Removal of Inorganic and Organic Hazardous Substances from Water: A Review,"* Molecules, 30 (2025) 554.

17. M. R. Oliveira, A. F. Silva, L. H. Santos, "Microwave-Assisted Synthesis of Zeolite A from Metakaolinite for CO_2 Adsorption," International Journal of Molecular Sciences 24 (2023) 14040.

CONTENTS

TECHNICAL SCIENCES: COTTON, TEXTILE AND LIGHT INDUSTRY

TECHNICAL SCIENCES: AGRICULTURE AND FOOD TECHNOLOGIES

CHEMICAL SCIENCES